

DIELECTRIC PROPERTIES OF NEMATIC LIQUID CRYSTAL MODIFIED WITH DIAMOND NANOPARTICLES

S. TOMYLKO,¹ O. YAROSHCHUK,¹ O. KOVALCHUK,¹ U. MASCHKE,²
R. YAMAGUCHI³

¹Institute of Physics, Nat. Acad. of Sci. of Ukraine
(6, Prosp. Nauky, Kyiv 03680, Ukraine; e-mail: tomulkosv@ukr.net)

²Laboratoire de Chimie Macromoleculaire, CNRC,
Universite des Sciences et Technologies de Lille
(Villeneuve d'Ascq Cedex, France)

³Department of Electrical and Electronic Engineering, Akita University
(Tegatagakuen-cho, Akita, Japan)

PACS 77.22.-d, 61.30.-v,
81.05.uj
©2012

In the present study, the influence of diamond nanoparticles (DNPs) on dielectric properties of nematic liquid crystal (LC) E7 from Merck has been considered. It is established that the insertion of DNPs leads to an increase in the dielectric constant ϵ' , as well as to a significant change in the electric conductivity σ of the LC. The growth of ϵ' with the concentration of DNPs, C_{DNP} , is mainly caused by a contribution of the DNP permittivity to the effective permittivity of the composite. The character of the $\sigma(C_{\text{DNP}})$ curves depends on the ionic purity of LC E7: for the samples based on pure E7, an increase of the electric conductivity with the concentration of DNPs is detected, whereas the reverse trend is observed for the samples containing impure E7. This behavior is attributed to the competitive adsorption and desorption of ions on/from the surface of DNPs and the ion transfer along the percolation network of these particles.

1. Introduction

In recent years, composite systems based on liquid crystals (LCs) and nanoparticles have been intensively investigated. Such interest is caused by a possibility of extending the range of properties of LCs and reducing the parasitic effects typical of electro-optical devices based on LC layers. In these studies, magnetic [1], ferroelectric [2], dielectric [3], semiconducting [4] and metal [5] nanoparticles have been used as LC fillers. As a result, the essential change of viscoelastic, dielectric, optical, electro- and magneto-optical properties of LC matrices has been achieved [6].

One of the most intriguing classes of the fillers is formed by carbonaceous materials including such unique objects as carbon nanotubes (CNTs) [6–8]. Because of their elongated shape and a molecular structure similar to that of LC, the carbon nanotubes can be eas-

ily built into an orientationally ordered LC matrix [7, 8]. On the other hand, CNTs bring a number of improvements to LC layers used in electrooptical devices such as a reduction of the response time and the driving voltage and the suppression of the parasitic backflow and the image sticking [6, 9–11]. Besides influencing the intrinsic properties of LCs, CNTs result in new effects. One of them is the effect of electrooptical memory caused by the stabilization of a field-induced alignment of LC by a continuous network of CNTs formed in this state [6]. The stabilizing effect comes from the effective interaction of LC with the CNT network, which is partially aligned together with the LC host in an electric field. The CNT network reveals itself in a sharp increase of the conductivity of LC-CNTs dispersions with the concentration of CNTs.

In the present work, we investigate LCs filled with nanoparticles of diamond (DNPs), which is a different allotropic form of carbon. In contrast to multiwalled CNTs with the quasimetallic conductivity (along the tube axis), DNPs are non-conductive. At the same time, the NPs of diamond are characterized by huge values of dielectric permittivity: the dielectric constant of these particles dramatically increases during the transition from macro- to nanosize (from 5.75 (macrosize) to 7×10^4 ($d \sim 4$ nm)) that, as believed, is due to the adsorption and efficient clustering of water on the particles' surface [12]. The influence of DNPs on the permittivity and the conductivity of LC is mentioned in our recent work [13].

The present work is a logical extension of work [13]. It brings a number of new results that give an opportunity to establish unequivocally the reasons for the changes

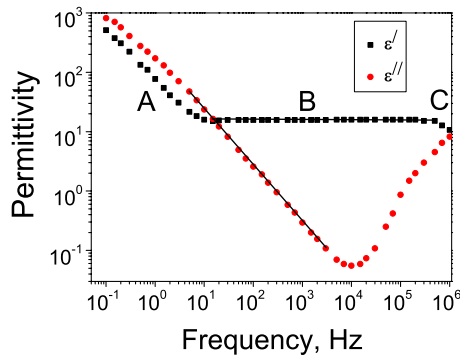


Fig. 1. Frequency dependences of the real ϵ' and imaginary ϵ'' parts of the complex dielectric constant for E7 sample at 20 °C

of the dielectric parameters of LC with the insertion of DNPs.

2. Experimental Section

2.1. Materials and samples

As a host material, we used nematic liquid crystal mixture E7 from Merck with the dielectric anisotropy $\Delta\epsilon = 13.8$ and the clearing temperature 58 °C. We used two samples of this LC, purified and contaminated with ionic impurities appearing due to the long-time exposure of E7 to air. As an LC filler, we used DNPs from Aldrich in a form of quasispherical particles with an average size of 10 nm [14]. The LC was mixed with particles by an ultrasonic mixer UZDN-2T (Russia). The mixing time was 10 min. A series of samples with concentrations of DNPs, C_{DNP} , equal to 0, 0.25, 0.5, 1, 2, and 4 wt.% has been investigated.

The glass substrates with transparent conductive indium tin oxide (ITO) coatings and aligning polyimide layers were used for assembling the liquid crystal cells. We utilized polyimides AL3046 (JSR, Japan) and SE1211 (Nissan, Japan) for the planar and homeotropic LC alignments, respectively. The polyimide layers were unidirectionally rubbed by a fleecy cloth. The cells were assembled so that the rubbing directions of different substrates were antiparallel (antiparallel cells). The thickness of the cells was set by 20 μm glass spacers. These cells were filled with pristine LC or LC doped with DNPs.

2.2. Methodology of dielectric measurements

The equivalent circuit of an LC cell consists of parallel connected resistance R and capacity C . By using the oscilloscopic method [15, 16], these parameters were mea-

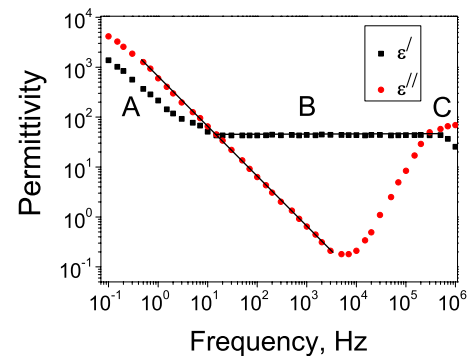


Fig. 2. Frequency dependences of the real ϵ' and imaginary ϵ'' parts of the complex dielectric constant for an E7-DNPs (2 wt.%) sample at 20 °C

sured as functions of the frequency of a sine-like testing electric field applied across the LC cell. The amplitude of the measured signal was 0.25 V. The frequency f was varied within the range $5 \times 10^{-2} - 10^6$ Hz. Using the measured data for R and C , the real ϵ' and imaginary ϵ'' parts of the permittivity were calculated. As an example, Figs. 1 and 2 present the $\epsilon'(f)$ and $\epsilon''(f)$ plots for pure LC E7 and for E7 doped with 2 wt.% of DNPs, respectively.

The values of ϵ'' were used to determine the sample conductivity σ according to the formula

$$\sigma = 2\pi f \epsilon_0 \epsilon'' \quad (1)$$

where ϵ_0 is the electric constant. For this estimation, the frequency $f = 100$ Hz was used. It corresponds to the linear part of the double logarithmic plot of $\epsilon''(f)$ curves (Figs. 1 and 2) implying the frequency independence of the conductivity. This allowed us to attribute the measured conductivity to the ionic conductivity of LC. The dielectric constant ϵ' was also estimated for $f = 100$ Hz corresponding to the plateau of the $\epsilon'(f)$ curve.

Dielectric measurements were carried out for planar and homeotropically aligned layers of the suspensions at room temperature and the temperature 80 °C corresponding to the nematic and isotropic phases, respectively.

3. Experimental Results and Discussion

At first, the dielectric spectra $\epsilon'(f)$ and $\epsilon''(f)$ have been measured and analyzed. As an example, Figs. 1 and 2 demonstrate the $\epsilon'(f)$ and $\epsilon''(f)$ curves for planar-aligned layers of E7 and E7-DNP dispersion ($C_{\text{DNP}} = 2$ wt.%), respectively, which are typical of these series. As one can see, three parts of the spectra can be

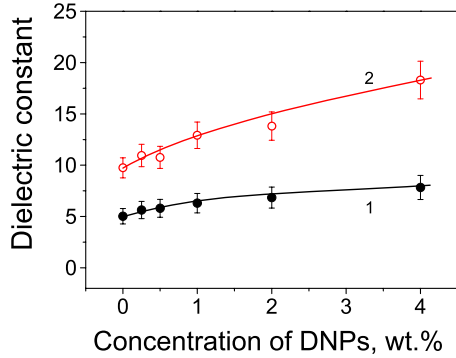


Fig. 3. Permittivity of planar aligned LC E7-DNPs samples as a function of the DNP concentration. Curves 1 and 2 correspond to 20 °C and 80 °C, respectively

distinguished. Part A ($f < 10$ Hz) corresponds to the low-frequency relaxation. It is determined by the near-electrode processes and particularly by the charge exchange between the electrode and ions presented in the liquid [17]. Part B ($f = 10 - 5 \times 10^3$ Hz) characterizes bulk properties of the sample, namely, the polarization and the charge transfer in the LC bulk. The second relaxation process (part C, $f > 10^4$ Hz) is commonly assigned to the dipole relaxation associated with rotations around the short molecular axis [18]. The collective character of molecular rotations in LCs explains the essential fall of the frequency of this relaxation comparing with isotropic liquids.

Comparing the data for pure and DNP doped LC E7, one can notice that the insertion of DNPs results in shifting the $\varepsilon'(f)$ and $\varepsilon''(f)$ curves to lower frequencies that implies slowing down the relaxation processes. Apparently, the nanoparticles impede the rotation of LC molecules and influence the ionic concentration. One can also notice an increase of the dielectric constant ε' in the whole frequency range investigated in this work.

Curve 1 in Fig. 3 shows the dependence of the dielectric constant ε' on the concentration of DNPs, C_{DNP} , obtained for the planar-aligned composites at the temperature of the nematic phase. There is obvious that ε' monotonically grows with C_{DNP} . Such a growth in the planar-aligned samples can be caused by two reasons. The first of them is the disordering of LC and thus an increased contribution of the parallel component of the dielectric constant of LC, $\varepsilon'_{\text{LC}\parallel}$, to the measured permittivity ε' of the composite. The second reason involves the mixing of dielectric constants of LC and DNPs, which can be expressed with the formula

$$\varepsilon' = \varphi_{\text{LC}}\varepsilon'_{\text{LC}} + \varphi_{\text{DNP}}\varepsilon'_{\text{DNP}}, \quad (2)$$

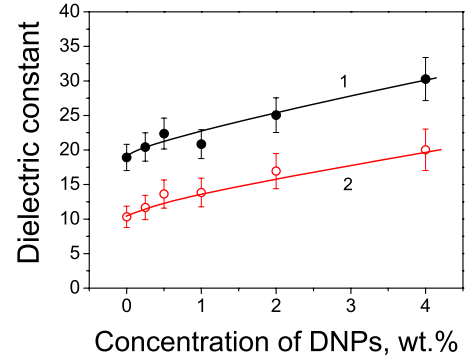


Fig. 4. Permittivity of homeotropically aligned LC E7-DNPs samples as a function of the DNP concentration. Curves 1 and 2 correspond to 20 °C and 80 °C, respectively

where φ_{LC} and φ_{DNP} are volume fractions of LC and DNPs.

In previous work [13], we assumed that the primary role is played by the first process. Our assumption was based on the fact that ε' at the maximal concentration of DNPs used in the work approximated $\langle \varepsilon'_{\text{LC}} \rangle = \frac{1}{3}(\varepsilon'_{\text{LC}\parallel} + 2\varepsilon'_{\text{LC}\perp})$ corresponding to the fully disordered state. In favor of this assumption, the estimate for ε' made for low C_{DNP} in frame of the Maxwell–Wagner effective medium theory [19] was few orders of magnitude lower than the experimentally measured values.

In the following, few facts cast doubt on this assumption. It became clear that, for determining the dominant mechanism, it is necessary to create the conditions, under which one of these mechanisms is eliminated or these mechanisms lead to opposite changes in the dielectric constant. Because of this, the further measurements were carried out in the isotropic phase, where the mechanism associated with the LC disordering is absent.

In this state, the increasing dependence $\varepsilon'(C)$ was also observed (curve 2, Fig. 3). Since the disordering contribution is missing, this increase can be entirely attributed to the contribution of DNPs to the overall permittivity of the composite. This conclusion is additionally confirmed by the experiments conducted for a cell with homeotropic alignment. In this configuration, the $\varepsilon'(C_{\text{DNP}})$ curve should decrease, starting from $\varepsilon'_{\text{LC}\parallel}$ and approaching $\langle \varepsilon'_{\text{LC}} \rangle$ at high concentrations of DNPs, if the disordering mechanism dominates. However, in the experiment, the opposite behavior was observed; the $\varepsilon'(C_{\text{DNP}})$ curve demonstrated a growth in the nematic, as well as in the isotropic phase (Fig. 4). It should be noted here that the growing of ε' by adding nanoparticles was earlier observed for a number of liquid and solid organic compounds [20, 21]. For liquid crystals, this ef-

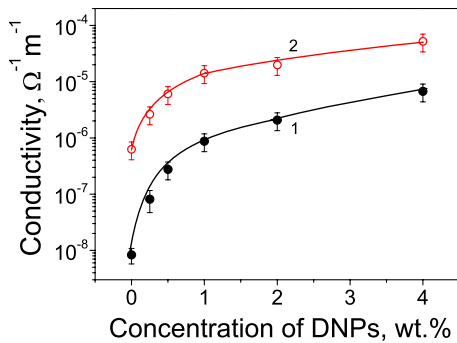


Fig. 5. Conductivity of planar aligned LC E7-DNPs samples based on pure LC E7 as a function of the DNP concentration. Curves 1 and 2 correspond to 20 °C and 80 °C, respectively

fect was described for LC suspensions of nanoparticles of ferroelectric materials [22].

Based on Eq. (2), the permittivity of DNPs can be estimated. We make this estimate for the isotropic state to avoid errors caused by the disordering of LC. According to curve 2 of Fig. 3, for $C_{\text{DNP}} = 0.02$ ($\varphi_{\text{DNP}} = 0.007$), $\varepsilon' = 15$. By setting $\varepsilon' = 15$, $\varepsilon'_{\text{LC}} = 10$, $\varphi_{\text{DNP}} = 0.007$, and $\varphi_{\text{LC}} = 0.993$ in (2), one can obtain $\varepsilon'_{\text{DNP}} = 750$. It should be noted that the evaluation of $\varepsilon'_{\text{DNP}}$ according to formula (2) gives its minimum value, since the formula does not take into account the polarization effects at the boundaries of particles. But even this minimal estimate is striking in its greatness. This value is in rather good agreement with the data obtained in [12]. According to the dependence of $\varepsilon'_{\text{DNP}}$ on the particle diameter d presented in this work, the value $\varepsilon'_{\text{DNP}} = 750$ corresponds to $d \approx 25$. The last estimate is rather close to the averaged size of DNPs provided by the producer [14].

The $\sigma(C_{\text{DNP}})$ curves for the planar-aligned composites based on pure LC E7 are presented in Fig. 5. These curves demonstrate a monotonic growth. This growth is rather rapid at the initial stage that might reflect some percolation process. Also, the conductivity grows with the temperature that might reflect an increase of the charge carrier mobility and the concentration of free ions [23, 24]. A similar behavior is observed for the same composites in the cells with homeotropic anchoring.

At the same time, the surprising results were obtained for the samples based on impure LC E7. For these samples, in contrast to the data above, the $\sigma(C_{\text{DNP}})$ curve monotonically decreases (Fig. 6). This result suggests that DNPs effectively rectify LC with strong ionic contamination, which was previously observed for other types of nanoparticles [25, 26]. Different behavior of

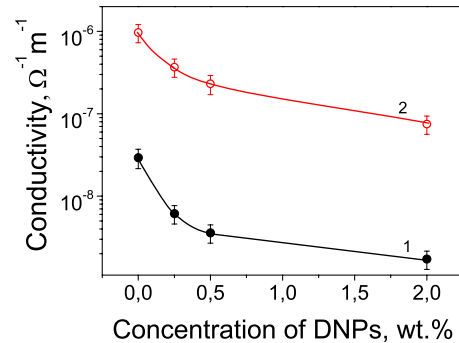


Fig. 6. Conductivity of planar aligned LC E7-DNPs samples based on impure LC E7 as a function of the DNP concentration. Curve 1 and curve 2 correspond to 20 °C and 80 °C, respectively

$\sigma(C_{\text{DNP}})$ curves for the samples based on pure and impure LC can be explained by different ratios of the ionic adsorption/desorption processes at the nanoparticle surface. Increasing the $\sigma(C_{\text{DNP}})$ curve might be caused by the prevailing desorption of an ionic impurity from the surface of DNPs into the LC and the ion transfer along the surface of interconnected particles. In turn, the opposite trend suggests that the adsorption of ionic impurities from LC E7 on the surface of DNPs dominates.

4. Conclusions

We demonstrate that the insertion of diamond nanoparticles in the nematic liquid crystal E7 substantially modifies its dielectric properties. Such a doping essentially increases the permittivity of LC layers mainly due to adding the properties of DNPs to the LC. Due to the high permittivity of DNP ($\varepsilon'_{\text{DNP}} = 10^2\text{--}10^3$ [12]), even small (1–4 wt.%) fractions of DNPs result in the increase of the effective permittivity of LC-DNPs composites by a factor of two and more. The change in the conductivity, when adding the nanoparticles, depends on the concentration of free ions in LC E7. For pure LC, the conductivity grows with the loading of DNPs, while, for the E7 probes enriched with ions, the reverse trend is observed. In the latter case, one can say about a significant ion purification of LC. Different trends for the ionically pure and impure samples can be explained by different relationships of the processes of ionic adsorption and desorption at the nanoparticle surface. Moreover, to accurately describe the shape of $\sigma(C_{\text{DNP}})$ curves, the conductivity percolation due to the formation of a DNP network should be taken into account.

O.V.Y. acknowledges the financial support from Japan Society for Promotion of Science under grant No. L-10535.

1. S.-H. Chen and N.M. Amer, Phys. Rev. Lett. **51**, 2298 (1983).
2. F. Li, O. Buchnev, C.I. Cheon *et al.*, Phys. Rev. Lett. **97**, 147801 (2006).
3. G.Ya. Guba, Yu.A. Reznikov, N.Yu. Lopukhovich, V.M. Ogenko, V.Yu. Reshetnyak, and O.V. Yaroshchuk, Mol. Cryst. Liq. Cryst. **251**, 303 (1994).
4. T. Zhang, C. Zhong, and J. Xu, Jpn. J. Appl. Phys. **48**, 055002 (2009).
5. Y. Shiraishi, N. Toshima, K. Maeda *et al.*, Appl. Phys. Lett. **81**, 2845 (2002).
6. L. Dolgov, S. Tomylko, O. Koval'chuk, N. Lebovka, and O. Yaroshchuk, in *Carbon Nanotubes* (In-Tech., Vukovar, Croatia, 2010). Available from: <http://sciyo.com/books/show/title/carbon-nanotubes>.
7. J. Lagerwall and G. Scalia, J. Mater. Chemistry **18**, 2890 (2008).
8. M. Rahman and W. Lee, J. Phys. D: Appl. Phys. **42**, 063001 (2009).
9. W. Lee, C.-Y. Wang, and Y.-C. Shih, Appl. Phys. Lett. **85**, 513 (2004).
10. I.-S. Baik, S.Y. Jeon, S.H. Lee, K.A. Park, S.H. Jeong, K.H. An, and Y.H. Lee, Appl. Phys. Lett. **87**, 263110 (2005).
11. H.-Y. Chen and W. Lee, Appl. Phys. Lett. **88**, 222105 (2006).
12. S.M. Gavrilkin, K.B. Poyarkov, B.V. Matseevich, and S.S. Batsanov, Inorg/ Mater/ **45**, 980 (2009).
13. S. Tomylko, O. Yaroshchuk, O. Kovalchuk, U. Maschke, and R. Yamaguchi, Mol. Cryst. Liq. Cryst. **541**, 273 (2011).
14. <http://www.sigmaaldrich.com/catalog/ProductDetail.do?N4=636444|ALDRICH&N5=SEARCH CONCAT PNO|BRAND KEY&F=SPEC&lang=en US>.
15. A.J. Twarowski and A.C. Albrecht, J. Chem. Phys. **20**, 2255 (1979).
16. A.V. Koval'chuk, Funct. Mater. **5**, 426 (1998).
17. A. Sawada, K. Tarumi, and S. Naemura, Jpn. J. Appl. Phys. **38**, 195 (1999).
18. L.M. Blinov and V.G. Chigrinov, *Electrooptics Effects in Liquid Crystal Materials* (Springer, New York, 1996).
19. http://en.wikipedia.org/wiki/Effective_medium_approximations.
20. Z. Chen, K.-S. Zhao, L. Guo, and C.-H. Feng, J. Chem. Phys. **126**, 164505 (2007).
21. Ta.-I. Yang and P. Kofinas, Polymer **48**, 791 (2007).
22. E. Ouskova, O. Buchnev, V. Reshetnyak, Yu. Reznikov, and H. Kresse, Liq. Cryst. **30**, 1235 (2003).
23. A. Sawada, K. Tarumi, and S. Naemura, Jpn. J. Appl. Phys. **41**, 195 (2002).
24. S. Murakami and H. Naito, Jpn. J. Appl. Phys. **36**, 2222 (1999).
25. H.-Y. Chen and W. Lee, Appl. Phys. Lett. **88**, 222105 (2006).
26. H. Liu and W. Lee, Appl. Phys. Lett. **97**, 023510 (2010).

Received 28.09.11

ДИЕЛЕКТРИЧНІ ВЛАСТИВОСТІ НЕМАТИЧНОГО РІДКОГО КРИСТАЛА, МОДИФІКОВАНОГО АЛМАЗНИМИ НАНОЧАСТИНКАМИ

С. Томилко, О. Ярошук, О. Ковальчук,
У. Машке, Р. Ямагучі

Резюме

У роботі розглянуто вплив алмазних наночастинок (АНЧ) на діелектричні властивості нематичного рідкого кристала (РК) E7 фірми Мерк. Встановлено, що додавання АНЧ приводить до збільшення діелектричної проникності ϵ' , а також до значної зміни провідності σ рідкого кристала. Зростання ϵ' з концентрацією АНЧ, $C_{\text{ДНР}}$, головним чином, пов'язане з внеском діелектричної проникності АНЧ в ефективну проникність композиції. Поведінка кривих $\sigma(C_{\text{ДНР}})$ залежить від чистоти РК E7: для зразків на основі чистого E7 виявлено зростання електричної провідності, тоді як для зразків з домішковим E7 спостерігалась зворотна тенденція. Така поведінка пояснюється конкуренцією процесів адсорбції та десорбції іонів на/з поверхні АНЧ та переносом іонів по поверхні перколяційної сітки цих частинок.